IR spectroscopy of ethanol in nitrogen cryomatrices with different concentration ratios

A. Aldiyarov, M. Aryutkina, A. Drobyshev, and V. Kurnosov

Citation: Low Temp. Phys. **37**, 524 (2011); doi: 10.1063/1.3622633
View online: http://dx.doi.org/10.1063/1.3622633
View Table of Contents: http://ltp.aip.org/resource/1/LTPHEG/v37/i6
Published by the American Institute of Physics.

IR spectroscopy of ethanol in nitrogen cryomatrices with different concentration ratios

A. Aldiyarov, M. Aryutkina, A. Drobyshev,[a] and V. Kurnosov

Al-Farabi Kazakh National University, Almaty 050038, Kazakhstan
(Submitted October 28, 2010; revised December 9, 2010)
Fiz. Nizk. Temp. **37**, 659–669 (June 2011)

Thin films of cryovacuum condensates of ethanol-nitrogen mixtures formed by co-condensation of gas mixtures with different concentrations on a cooled metal substrate are studied by IR spectrometry. The condensation temperature was $T_c = 16$ K and the pressure of the gaseous phase during cryodeposition was $P = 10^{-5}$ Torr. The ethanol concentration in nitrogen was varied from 0.5 to 10% and the film thickness, from 1 to 30 μm. Measurements were made in the range from 400 to 4200 cm^{-1}. An analysis of the IR spectra and a comparison with published data shows that ethanol monomers and dimers are present in the nitrogen matrix. This is indicated by an absorption band at a frequency of 3658 cm^{-1} owing to vibrations of O–H bonds of ethanol monomers and dimers. The local minima of this band at 3645 and 3658 cm^{-1} are related to the existence of two conformational states of the ethanol molecule: anti (3658 cm^{-1}) and gauche (3645 cm^{-1}). In addition, the presence of ethanol dimers and monomers in the matrix leads to the appearance of absorption bands at 1259 and 1276 cm^{-1} attributable to deformation vibrations δ(COH) of the anti- and gauche-isomers, respectively, as well as bands corresponding to a combination of ν(CCO) valence vibrations and rotational oscillations of the methyl group $r(CH_3)$ attributable to anti-dimers ($\nu = 1090$ cm^{-1}) and anti-monomers ($\nu = 1095$ cm^{-1}). Local minima within 3000–3600 cm^{-1} also indicate the presence of cyclical dimers, trimers, and tetramers, as well as hexamers in the matrix. A broad band over 3250–3330 cm^{-1} indicates that large polyaggregates, with ethanol molecules in a hydrogen-bond state (multimer), exist in the matrix. © *2011 American Institute of Physics*. [doi: 10.1063/1.3622633]

INTRODUCTION

For almost 90 years condensed states of ethanol have been an object of research on various levels and scales. Beginning with the work of Gibson[1] and through the present, researchers from various countries have studied the unique properties of solid ethanol using acoustic, optical, structural, calorimetric, and other techniques. This persistent attention is a result of the fact that ethanol has some extremely interesting polymorphic and polyamorphous properties. At temperatures below its melting point ($T_m = 159$ K), ethanol exists in various states: a glassy state (structured glass SG), formed during rapid cooling of the liquid phase to temperatures below the glass transition temperature $T_g = 97$ K; a plastic crystal (PC, bcc), formed via an intermediate supercooled liquid (SCL) phase by heating the SG above T_g; an orientationally disordered crystal (ODC), formed by cooling of the plastic crystal to temperatures below 97 K; and a monoclinic crystalline (MC) state that is the basic stable state of solid ethanol. Rigorous studies over the last few decades have yielded a state diagram for solid ethanol.[2–5] Usually, the glassy state of ethanol is produced by ultrafast cooling (quenching) with subsequent thermally stimulated transformations. But there is another obvious way of producing an amorphous state, including the structured glass: condensation from the gaseous state onto a substrate that has been cooled to below the glass transition temperature. We believe that this approach is the best controlled experimental technique from the standpoint of the rate and degree of supercooling.

We have recently carried out a cycle of studies of the thermally stimulated conversion of various gases (including water vapor and ethanol) into cryovacuum condensates.[6–8] These studies have addressed the role of cluster formation processes in the formation of thin cryocondensate films on cooled surfaces. It was assumed that these processes have a significant effect on the formation of the near ordering structure of cryocondensates and, therefore, on the character of their subsequent thermally stimulated transformations. To do this, we have used a cryomatrix isolation technique with nitrogen as the cryomatrix. The results on the cryodeposition of water vapor are discussed in Ref. 9. A natural next step in this area is to conduct similar studies of cryocondensation processes in ethanol. On the whole, these studies used the same apparatus and techniques as the earlier work,[9] with some distinctive features to be discussed below.

STATEMENT OF THE PROBLEM AND EXPERIMENT

Our task in these studies was to try to explain the complicated and often nonunique behavior of thin cryocondensate films of ethanol in the course of thermally stimulated transformations in terms of the effect of the cluster composition of these deposits on these transformation processes. To do this, we studied the cryodeposition of gaseous ethanol-nitrogen mixtures with different concentration ratios, as well as the properties of the resulting cryocondensates. The object of study was thin films of nitrogen (matrix) cryocondensate that contain ethanol molecules in various cluster states. Varying the concentration of ethanol in the nitrogen should lead to changes in the cluster composition of the ethanol molecules immobilized in the nitrogen matrix.

Our analysis of the spectra we obtained for determining the cluster composition of ethanol in the nitrogen matrix is based on comparisons with published data. Of the large number of related studies, theoretical, as well as experimental, we have chosen papers that used two methods for producing

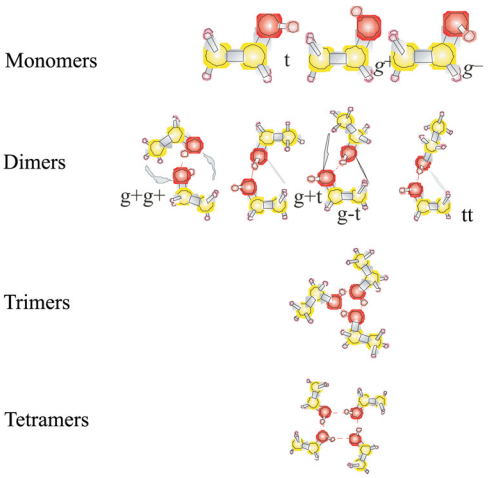

3685, 3678, 3660 [11]; 3661 [12]; 1446 (t), 1094 (t), 1275 (g), 2988 (g), 1261 (t), 882 (g) [20]; 3645 (g),3658 (a) [10]

3672, 3654, 3548, 3542, 3540, 2984 (tt) [11]; 3547, 3540, 3532 [12]; 1445 (tt), 2983 (tg), 1489 (tg), 1464 (tt), 2984 (tt), 2983 (tg), 1056 (tg), 883 (tg), 811 (tg), 418 (tt) [13,20]; 3537 (cycl.), 3576 (cycl.), 3645 (g) [10]

3447 [12]; 3433 [13] 2984 (ttt), 1464 (ttt) [20] 3432 (cycl.), 3487 (cycl.) [10]; 3433 [13];

3378 (cycl.), 3402 (cycl.) [10]; 3378 [13]

FIG. 1. Major types of ethanol polyaggregates, the principles for their formation, and their manifestations in different spectral regions. Notation: (t) trans, (g) gauche-conformal, (a) anti-conformal, (cycl.) cyclical cluster. The units corresponding to the numerical values are cm^{-1}.

the ethanol clusters: expansion of an He or He/Ne supersonic ethanol-containing jet[10–12] or co-condensation of ethanol with nitrogen as a matrix.[13–17] Thus, we have attempted to account for the fact that the clusters in a matrix can be formed in the gaseous phase with subsequent capture by the matrix or during condensation of a mixture, most likely in an adsorbed layer. We have used a generalization of the data from those studies for analyzing our spectra. Figure 1 shows the main types of ethanol polyaggregates, the way they are produced, and their spectral manifestations in various spectral ranges.

Some changes in technique have been made in the present work compared to Ref. 9, primarily in the method of preparing the nitrogen-ethanol mixture. In Ref. 9 the components are fed in parallel into the chamber using two calibrated leak valves. This made it unnecessary to account for separation of the mixture during injection, but it also meant that the concentrations of the components could not be measured with the needed accuracy. Studies show that any possible separation of the mixture during injection clearly makes a smaller contribution to the error in determining the concentration than the error owing to the need to measure the pressures of the mixture components during injection and then calculate the concentrations based on these measurements. Thus, we used a technique involving preparation of a mixture with a specified concentration in advance and injecting it into the chamber through a single leak valve. The rate of condensation and the thickness were monitored with a two-beam laser interferometer. After deposition of a film with a specified thickness, the gas feed was shut off and the IR reflection spectra of the film-substrate were measured. The main experimental parameters were: substrate temperature $T=16$ K, mixture injection pressure $P=10^{-5}$ Torr, ethanol concentration in nitrogen from 0.5 to 10%, and, frequency range of the spectra from 4200 to 400 cm^{-1}.

RESULTS AND DISCUSSION

Figure 2 shows the vibrational spectra of thin films of nitrogen-ethanol cryocondensates with different ethanol concentrations. The frequency range was 4200–400 cm^{-1}. The condensation temperature for the samples was 12 K. The sample thicknesses were set in accordance with the concentrations of ethanol in the nitrogen matrix: $d=5$ μm for $C=10\%$; $d=7.5$ μm for $C=5\%$; $d=10$ μm for $C=3\%$; $d=10$ μm for $C=1.5\%$; and, $d=12.5$ μm for $C=0.5\%$. Thus, as the ethanol concentration was reduced, the film thickness was increased, so that the number of ethanol molecules interacting with the radiation from the globar did not vary significantly with the different concentrations. In addition, for convenience in the analysis and comparison of the spectra obtained at different ethanol concentrations, the corresponding data bases are multiplied by a constant. The following notation is used in the figure: ν(OH) valence vibrations of O–H bonds; ν(CH) valence vibrations of C–H bonds; $\delta(CH_3, CH_2)$ deformation vibrations of methyl and methylene groups; $\delta+\nu+r$(CH) combined deformation, valence, and radiating (fan) vibrations; and, ν(CO) valence vibrations of C–O bonds. For a more detailed discussion of these results, it is appropriate to subdivide the range of frequencies into intervals corresponding to the characteristic vibrations of the ethanol molecule.

The 3000–3700 cm^{-1} interval corresponds to valence vibrations of O–H bonds in free and bound states of the molecules. The frequency range from 2800 to 3000 cm^{-1} corresponds to symmetric and asymmetric valence vibrations of C–H bonds in methyl CH_3 and methylene CH_2 groups. The 1300–1500 cm^{-1} interval covers the frequencies of deformation and radiating vibrations of CH_3 and CH_2 groups.

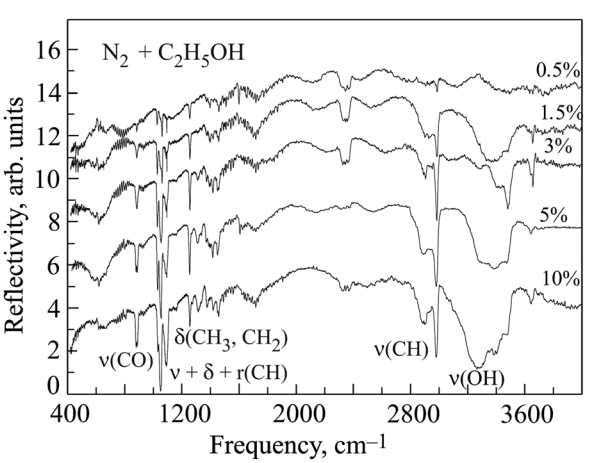

FIG. 2. Vibrational spectra of thin cryocondensate films of nitrogen-ethanol mixtures with different ethanol concentrations. The condensation temperature $T=12$ K. The sample thicknesses vary with the ethanol concentration: $d=5$ μm ($C=10\%$); $d=7.5$ μm ($C=5\%$); $d=10$ μm ($C=3$ and 1.5%); $d=12.5$ μm ($C=0.5\%$).

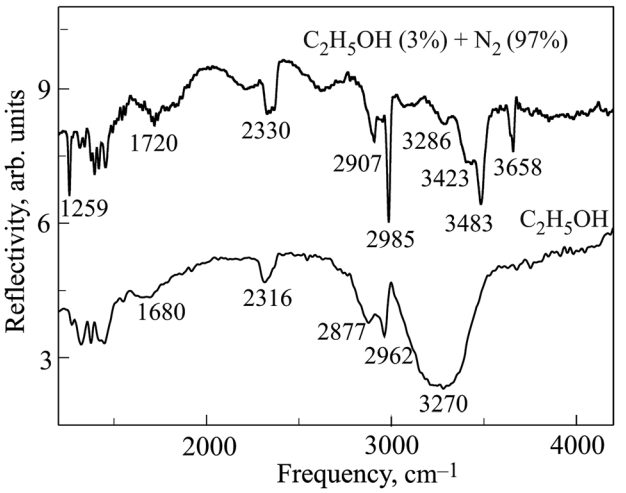

FIG. 3. Comparison of the vibrational spectra of thin cryocondensate films of pure ethanol and of an ethanol-nitrogen mixture. The upper curve is for a mixture of 3% ethanol and 97% nitrogen, condensation temperature $T = 12$ K, and sample thickness $d = 10$ μm. The lower curve is for ethanol, $T = 12$ K, and $d = 1$ μm. The frequencies corresponding to the absorption peaks in the main characteristic vibrations are indicated.

Combinations of valence, rotational, and vibrational frequencies lie in the range of 1200–1000 cm^{-1}. The absorption band in the 880–900 cm^{-1} frequency interval belongs to valence CCO-vibrations and their combinations with rotational oscillations of methyl and methylene groups. The band at 415–420 cm^{-1} corresponds to a deformation vibration along a CCO-bond.

It is appropriate to compare these data with IR spectra of pure films of ethanol samples with the same condensation temperature and thickness. Figure 3 shows comparison spectra for two samples, one a film of pure ethanol and the other a sample consisting of 3% ethanol and 97% nitrogen. The chosen ethanol concentration $C = 3\%$ contains all the characteristic features of a spectrum of ethanol in a nitrogen matrix relative to a pure sample. The thickness of the pure ethanol film was 1 μm and that of the mixture of ethanol and nitrogen was 10 μm. In accordance with the selected frequency ranges, we now examine the spectra in more detail.

1. The frequency interval 3000–3700 cm^{-1} corresponds to a valence O–H bond. The obvious difference is caused by a considerably lower degree of hydrogen bonding in the ethanol aggregates within a nitrogen matrix. The data of Fig. 1 show that the $\nu = 6358$ cm^{-1} absorption band can be interpreted as vibrations of O–H bonds of ethanol monomers and dimers. Its shift to longer wavelengths compared to the characteristic frequencies of monomers and dimers in the gaseous phase[11,12] appears to be caused by the influence of the nitrogen matrix lattice. Although a more detailed analysis of the interaction of the nitrogen lattice and ethanol molecules, as well as of the position of ethanol in the matrix, is of great interest, it is beyond the scope of the current study.

A more detailed examination of this band (Fig. 4) is of interest. As the figure shows, this band has local minima at $\nu = 3645$ and 3658 cm^{-1}. We assume that this is because of the existence of two conformational states of the ethanol molecule, anti (3658 cm^{-1}) and gauche (3645 cm^{-1}), owing to a difference in the positions and, therefore, the energies of hydrogen atoms in the O–H bond.[14–16] The figure shows that the difference in the energies of the conformers is 13 cm^{-1},

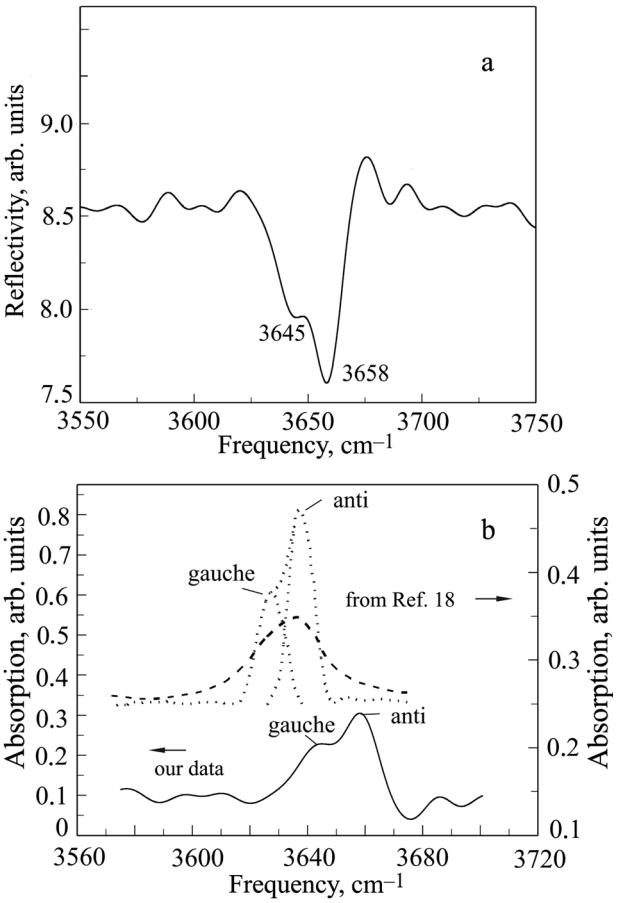

FIG. 4. (a) Spectral appearance of conformational features of the structure of the ethanol molecule. The local minima correspond to the anti (3658 cm^{-1}) and gauche (3645 cm^{-1}) isomers of ethanol with respect to the position of the hydrogen atom in the O–H bond. (b) Comparison with an IR spectral deconvolution of the asymmetric profile of the O–H bond absorption band.

in good agreement with published data.[15,17] In addition, the asymmetrical shape of this absorption band is consistent with the results[18] of an IR spectral deconvolution of the asymmetric absorption band profile of O–H bonds shown in Fig. 4(b). The slight difference in frequencies is a consequence of the nonuniformity of the cluster composition of ethanol in the nitrogen matrix, i.e., this band belongs to quasifree monomers or dimers of ethanol.

The O–H absorption band at 3000–3600 cm^{-1} (Fig. 5) also has local minima corresponding to different cluster compositions of ethanol molecules in the nitrogen matrix. Based on calculations and published experimental data,[13,19] we find that ethanol clusters of different sizes are present in the matrix. Figure 5 shows the frequencies of the local minima and their interpretations according to Ref. 20. The broad band at 3250–3330 cm^{-1} may mean that large polyaggregates, in which the ethanol molecules are in a hydrogen bonding state, appear in the matrix; these are indicated as multimers.

It should be noted that in the papers cited here, the aggregates larger than dimers are predominantly cyclical. The tendency of ethanol molecules to close hydrogen bonds cyclically, thereby forming the most stable clusters, may be the fundamental cause of the ability of ethanol to form stable polymorphic and polyamorphic (including glass) states.

2. The 2800–3000 cm^{-1} interval includes valence vibrations of CH bonds of methyl and methylene groups of ethanol. Figure 6 shows the vibrational spectra of films of pure

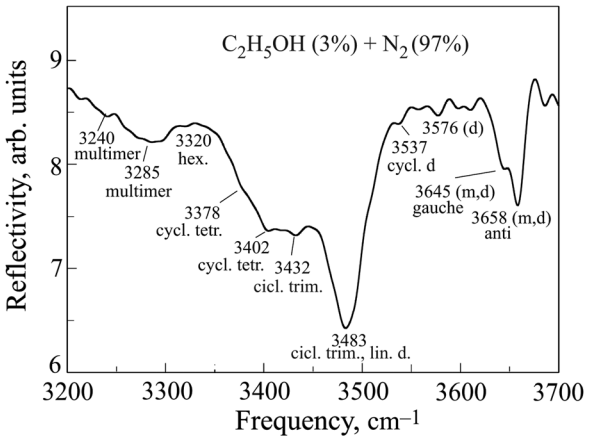

FIG. 5. Features of the absorption band of the O–H bond of ethanol (3%) in a nitrogen cryomatrix (97%). Notation: (m) monomer, (d) dimer, (cycl. d) cyclical dimer, (cycl. trim.) cyclical trimer, (cycl. tetr.) cyclical tetramer, (hex.) hexamer.

ethanol (a) and of a 3% mixture of ethanol in nitrogen (b) over this interval. One obvious difference is the finer structure of the spectrum attributable to ethanol states isolated by the matrix. The distinct narrow absorption peak at $\nu = 2985$ cm^{-1} is attributable to valence asymmetric vibrations of CH bonds of the methyl group $v_a(CH_3)$ in monomers and dimers.[20]

The faint band at $\nu = 2950$ cm^{-1} also is attributable to the same type of vibrations. The absorption band at $\nu = 2907$ cm^{-1} reflects CH-valence asymmetric vibrations of the methylene group, $v_a(CH_2)$, while the local extrema at 2894 and 2867 cm^{-1} correspond to a symmetric type of these oscillations.

Figure 6(a) shows an absorption spectrum in the range of the valence CH vibrations for a cryocondensate of pure ethanol. Compared to Fig. 6(b) there is a substantial broadening of the absorption bands; this causes the fine structure owing to the different types of molecular vibrations of ethanol to vanish. The two broad bands centered at 2962 and 2875 cm^{-1} correspond to valence vibrations of CH bonds of methyl and methylene groups, respectively.

Besides a broadening of the absorption bands, there is a substantial shift in their centers to low frequencies relative to Fig. 6(b). The shift is by $\Delta\nu = 23$ and 32 cm^{-1} for the methyl and methylene groups, respectively. The broadening of the CH valence vibrational bands and their "red" shift are both manifestations of intermolecular interactions of ethanol and of medium and long-range structural ordering of the cryocondensates.

3. The interval 1200–1500 cm^{-1} contains different kinds of deformation vibrations. Figure 7 shows the characteristic vibrational spectra of 3% ethanol in a nitrogen matrix (upper curve) and of a film of pure ethanol cryocondensate (lower curve) in more detail in this region with deformation (δ) and radiating (W) vibrations of ethanol, as well as combinations of these.

The structure of the 3% ethanol mixture is more complicated than that of the pure ethanol. Of the nine characteristic

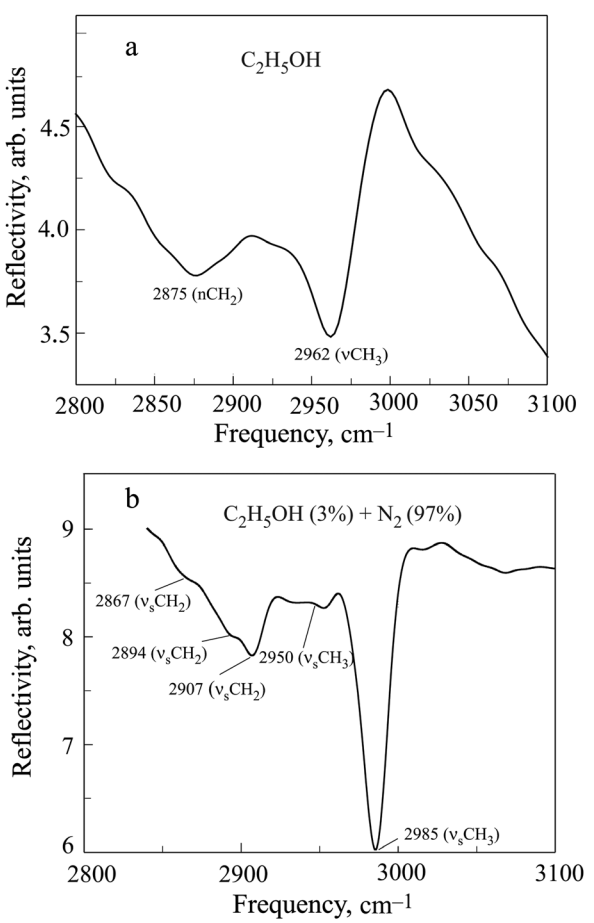

FIG. 6. Vibrational spectra of films of pure ethanol (a) and of a mixture of ethanol (3%) and nitrogen (97%) (b) over the range of frequencies of the valence vibrations of the CH-bond of ethanol.

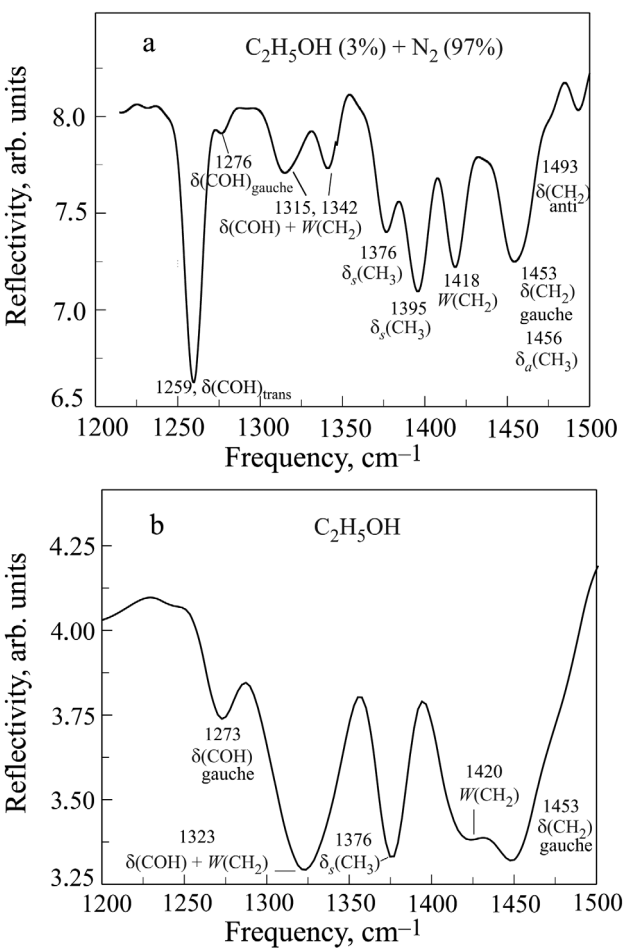

FIG. 7. Characteristic vibration frequencies of the ethanol molecule in a nitrogen matrix (3% + 97%) (a) and in a cryocondensate film of pure ethanol (b).

absorption peaks in the upper spectrum within this frequency range, only five remain in the spectrum of the pure film. The band at $\nu = 1493$ cm^{-1}, which corresponds to deformation vibrations of the methylene group $\delta(CH_2)$ in the anti-isomers, vanishes. The two separate bands of symmetric deformation vibrations of the methyl groups $\delta(CH)_s$ centered at 1376 and 1395 cm^{-1} appear to form a single band with a frequency $\nu = 1376$ cm^{-1} as they broaden. The same thing happens with the two separate frequencies (1315 and 1342 cm^{-1}) of a combination of deformation vibrations in the (COH) bond and radiating vibrations $W(CH_2)$ of methylene groups, and leads to the formation of a single broad band centered at $\nu = 1323$ cm^{-1}. The absorption band corresponding to deformation vibrations of the δ(COH) anti- and gauche-isomers at 1259 and 1275 cm^{-1} behaves in an interesting way. The band corresponding to anti-isomer vibrations of ethanol (1259 cm^{-1}) vanishes completely, while the gauche-isomer vibrations are retained and become more distinct. This effect seems to involve intermolecular formation of cyclical polyaggregates of ethanol with subsequent hindering of this type of vibrations in δ(COH) anti-bonds. We may assume that the δ(COH)-gauche bonds do not participate in the formation of ethanol molecular clusters.

As noted above, one of the clearest differences between these spectra is the absorption band at 1259 cm^{-1}. It is characteristic of δ(COH) deformation vibrations.[20] This band is entirely absent in the spectrum of the pure ethanol cryocondensate. Given the tendency of ethanol molecules to cyclical behavior in the formation of aggregates, this band should vanish for aggregates larger than dimers, since during formation of cyclical aggregates the vibrational degree of freedom for O–H bonds becomes impossible since it is involved in cluster formation. This assumption is supported by data from Ref. 20. Thus, this band can be attributed to the presence of ethanol monomers and dimers in the nitrogen matrix. This band also has two components (anti at 1259 cm^{-1} and gauche at 1276 cm^{-1}) that are manifestations of the conformal structure of the ethanol molecule.

4. The system of absorption bands within the frequency interval 1000–1120 cm^{-1} shown in Fig. 8 corresponds to combinations of valence ν(CCO) vibrations, $r(CH_3)$ and $r(CH_2)$ rotations of methyl and methylene groups, and δ(OH) deformation vibrations of OH bonds. The absorption spectrum of the ethanol-nitrogen mixture is more complicated than that of the pure ethanol cryocondensate. The 3% ethanol-nitrogen spectrum has three broad, distinct absorption peaks in this range, along with a sharp, narrow absorption band at $\nu = 1095$ cm^{-1}. The nature of the vibrations can be quite reliably established on the basis of published analyses.[12,14,17,18]

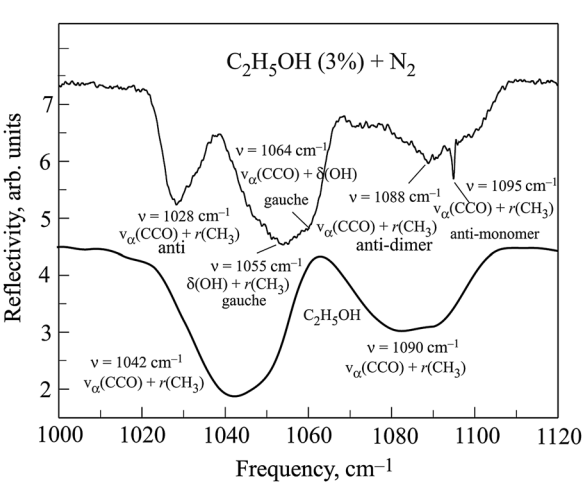

FIG. 8. Absorption spectra of a film of 3% ethanol in nitrogen and of pure nitrogen over the range of frequencies of combinations of ν(CCO) valence vibrations and rotations of methyl $r(CH_3)$ and methylene $r(CH_2)$ groups, as well as δ(OH) deformation vibrations of OH bonds.

The absorption band with a peak at $\nu = 1028$ cm^{-1} corresponds to a combination of ν(CCO) valence vibrations and $r(CH_3)$ rotation of the methyl group. This band is considerably wider in the case of the pure ethanol film and the center is shifted to $\nu = 1042$ cm^{-1}. Both are consequences of the interaction of ethanol molecules with the inner field of the lattice. The broad, distinct peak at $\nu = 1055$ cm^{-1} is associated with a combination of ν(CCO) valence vibrations and δ(COH) deformation vibrations of the COH bond. Here these vibrations are attributable to gauche conformal ethanol. Given the tendency to cyclical clustering on the part of ethanol molecules, the reduced amplitude of this vibration as the ethanol concentration in the nitrogen matrix increases and its complete disappearance in pure samples are understandable. Here the COH bonds participate in the formation of cyclical clusters and the "hindering" of this type of vibration.

The band centered at $\nu = 1090$ cm^{-1} is attributable to a combination of ν(CCO) valence vibrations and $r(CH_3)$ rotations of the methyl group. It has two characteristic peaks, associated with dimers (anti, $\nu = 1090$ cm^{-1}) and monomers (anti, $\nu = 1095$ cm^{-1}). Clearly, at this concentration, there is a substantial fraction of ethanol monomers in the nitrogen matrix.

There is some interest in how the cluster composition of the ethanol, especially the monomers, changes in the nitrogen matrix as the concentration ratio is varied. Vibrational spectra of ethanol at different concentrations in the nitrogen matrix are shown in Fig. 9. These curves show that, as the ethanol concentration is increased, there is a drop in the amplitude of the absorption band at $\nu = 1095$ cm^{-1}, which corresponds to a combination of ν(CCO) valence vibrations and $r(CH_3)$ rotation of anti-conformal methyl group monomers. Thus, the variation in the amplitude of this vibration is directly related to the variation in the concentration of ethanol monomers in the nitrogen matrix. This information is illustrated graphically below (in Fig. 11).

5. The frequency interval 800–1000 cm^{-1}. Figure 10 shows the absorption spectra of cryocondensate films of ethanol-nitrogen mixtures with different concentration ratios.

We examined the frequency interval corresponding to the ν(CCO) valence vibrations, as well as modes of combinations of these vibrations with rotation of the methyl group. The change in the spectrum with increasing ethanol concentration is noteworthy. Within the measured concentration interval of 0.5–3%, the absorption peak is an almost symmetric single band centered at $\nu = 885$ cm^{-1}. This band can be identified reliably as valence vibrations of the CCO bond.[17,18]

For the measured ethanol concentrations of 5 and 10% in nitrogen the band is observed to split with the appearance of two distinct minima with the same central frequencies for both concentrations, $\nu = 879$ and 888 cm^{-1}. The vibrations at $\nu = 879$ cm^{-1} can be interpreted as a combination of valence CCO vibrations and rotations of the methyl group in the M_g gauche-isomorph of the ethanol monomer.[17]

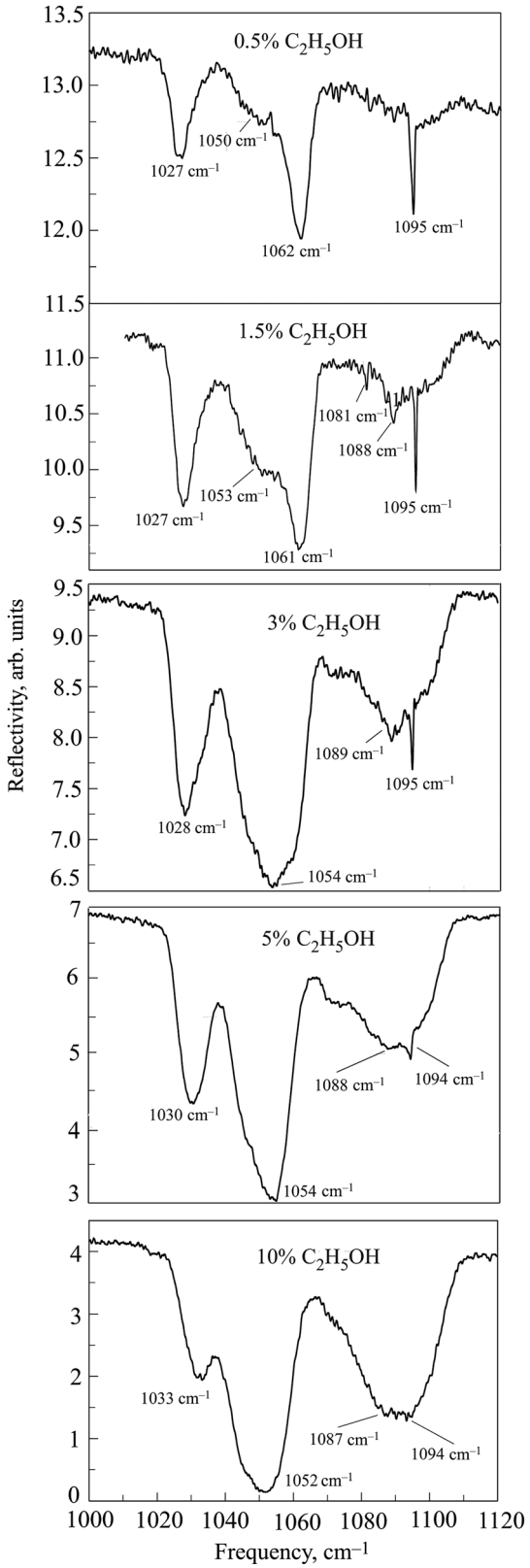

FIG. 9. Vibrational spectra of ethanol in nitrogen for different concentrations of ethanol.

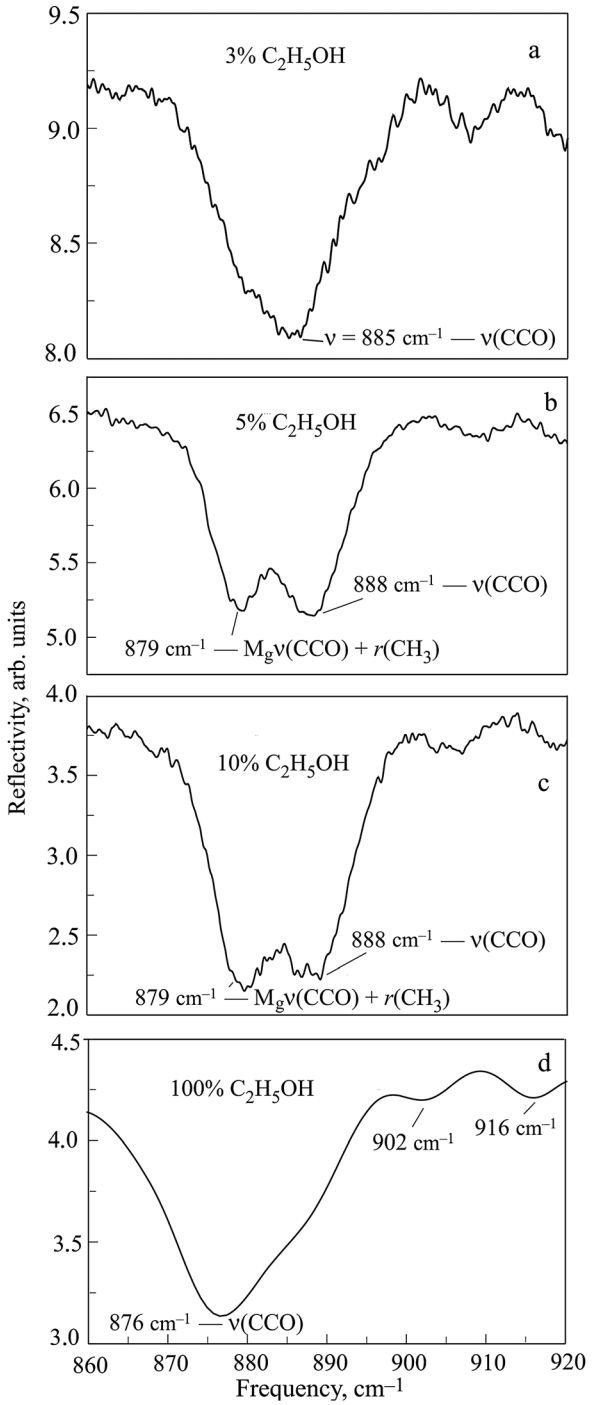

FIG. 10. Absorption spectra of ethanol-nitrogen cryocondensate films with different concentration ratios over the range of frequencies of the ν(CCO) valence vibrations and their combinations.

The relationship between the ethanol concentrations and the splitting of the CCO valence band observed at these concentrations is not entirely obvious. The data of Ref. 20 offer one possible interpretation. According to those data, the vibration frequencies for the monomers and dimers of ethanol are related as the ethanol concentration increases and cyclical clusters are formed. For aggregates larger than trimers, only the purely valence vibrations in the CCO bond remain, with three frequency modes (896, 898, and 900 cm^{-1}), which do not undergo splitting because the width of the absorption band in pure ethanol is so large.

The shift in the center of the absorption band to longer wavelengths is caused by the internal field in the 100% ethanol film sample. Nevertheless, it is not understood why this band has just one minimum (at $\nu = 884$ cm^{-1}) for concentrations of 0.5–3% and does not reflect the presence of monomers and dimers in these samples. We propose the following explanation for this: according to Ref. 20, the frequencies near those we have observed correspond to a combination of

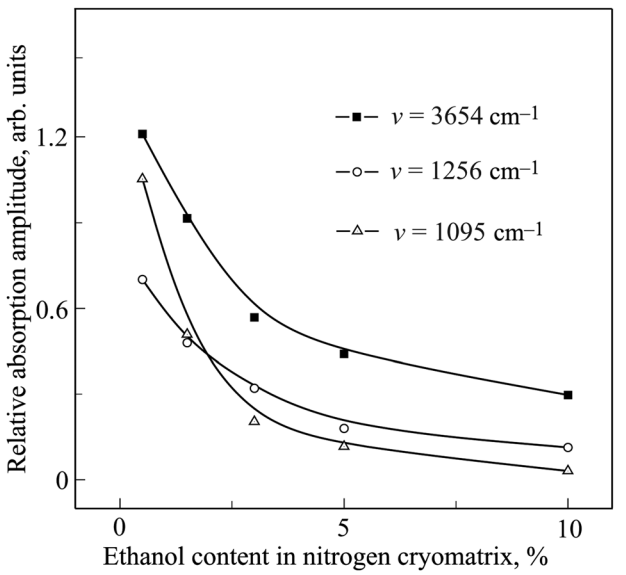

FIG. 11. Relative absorption amplitudes of characteristic vibrations of the ethanol molecule as functions of ethanol concentration in a nitrogen matrix. The amplitudes of these vibrations are normalized to the amplitude of the CH-bond of the methyl group at $\nu = 2985$ cm^{-1}.

valence and rotational transitions of the methyl group, $\nu(\mathrm{CCO}) + r(\mathrm{CH_3})$. Here the frequency $\nu = 896$ cm^{-1} corresponds to vibrations of the anti-monomer (or trans-, in the notation of Ref. 20). $\nu = 882$ cm^{-1} corresponds to vibrations of the gauche monomer, in full agreement with our experimental data (the center of the band lies at $\nu = 884$ cm^{-1}).

Assuming that it is mainly the anti-conformals which participate in the formation of cyclical polyaggregates makes it clear that these vibrations of the monomer are bound in the cycle, so that the band centered at $\nu = 884$ cm^{-1} belongs to gauche-monomer vibrations. Raising the ethanol concentration in nitrogen to 5–10% leads to a growth in the number of anti-gauche dimers D_{tg} with frequencies $\nu = 884$ and 900 cm^{-1}. Of these, the first corresponds to a symmetric valence vibration, when $\nu_s(\mathrm{CCO}_a)$ is an acceptor, while $\nu = 900$ cm^{-1} corresponds to a donor type of symmetric valence vibrations $\nu_s(\mathrm{CCO}_d)$. Further increases in the ethanol concentration lead to a sharp drop in the number of dimers, as well as of monomers, and the double absorption band degenerates into a single band.

As noted above, some of the characteristic vibrations of the ethanol molecule are correlated, to a high degree of reliability, with the presence of aggregates of different sizes in the nitrogen matrix. In particular, the absorption band at $\nu = 3658$ cm^{-1} (Figs. 3 and 4) corresponds to a valence O–H bond in monomers and dimers of ethanol. The peak at $\nu = 1259$ cm^{-1} (Figs. 7 and 8) is attributable to deformation vibrations of the O–H bond and also is an indication of the presence of monomers and dimers. And finally, the band at $\nu = 1095$ cm^{-1} corresponds to a combination of ν(CCO) valence vibrations and $r(\mathrm{CH_3})$ rotations of the methyl group, belonging to the anti-monomers ($\nu = 1095$ cm^{-1}). These three types of vibrations can, as a whole, characterize the amount of monomers and dimers in the matrix. In order to compare the different spectra for different concentrations, the amplitudes of these vibrations have been normalized to the amplitude of the CH bond of the methyl group at $\nu = 2985$ cm^{-1}, which is insensitive to changes in the ethanol concentration in the matrix. These data are shown in Fig. 11. All three of the curves behave similarly as the ethanol concentration is varied. This fact confirms our conclusions regarding the nature of the vibrations and their behavior.

CONCLUSIONS

1. An analysis of the IR spectra shows that ethanol monomers and dimers are present in the nitrogen matrix. This is indicated by the following:
   (a) the absorption band at 3658 cm^{-1} owing to O–H bond vibrations of ethanol monomers and dimers; the local minima in this band at 3645 and 3658 cm^{-1} are related to the existence of two conformal states of the ethanol molecule, anti (3658 cm^{-1}) and gauche (3645 cm^{-1});
   (b) the two absorption bands at 1259 and 1276 cm^{-1} attributable to δ(COH) deformation vibrations of the anti and gauche isomers, respectively; and,
   (c) the two bands corresponding to combinations of ν(CCO) valence vibrations and $r(\mathrm{CH_3})$ rotations of the methyl group belonging to anti-dimers ($\nu = 1090$ cm^{-1}) and gauche-monomers ($\nu = 1095$ cm^{-1}).
2. The local minima within the range 3000–3600 cm^{-1} indicate the presence, in the matrix, of the following ethanol aggregates: monomer, dimer, cyclical dimer, cyclical trimer, cyclical tetramer, and hexomer. The broad band over 3250–3330 cm^{-1} signifies the presence, in the matrix, of large polyaggregates with ethanol molecules in hydrogen bound states (multimers).
3. The local minima at 1259 and 1276 cm^{-1} are δ(COH) deformation vibrations of the anti- and gauche-isomers, respectively. The band corresponding to vibrations of the anti-isomer of ethanol (1259 cm^{-1}) vanishes completely as the ethanol concentration is raised, while the gauche-isomer vibrations are retained and become more distinct. This is explained by the fact that intermolecular formation of cyclical polyaggregates of ethanol occurs over the δ(COH) bonds with subsequent hindering of this type of vibration. Thus, it may be assumed that the δ(COH) gauche-bond does not participate in the formation of ethanol clusters.
4. The splitting of the valence CCO-vibration band as the ethanol concentration in the nitrogen matrix is changed (Fig. 11) is caused by coupling of the vibrations at the corresponding frequencies for ethanol monomers and dimers during the formation of cyclical clusters. For aggregates bigger than trimers, only the valence vibrations along the CCO bond with three frequency modes (896, 898, and 900 cm^{-1}) remain; these do not split because of the large width of the absorption band in pure ethanol samples. Raising the ethanol concentration to 5–10% leads to a growth in the number of anti-gauche dimers with frequencies $\nu = 884$ and 900 cm^{-1}. The first of these corresponds to a symmetric valence vibration of a (CCO_a) acceptor, while $\nu = 900$ cm^{-1} corresponds to a donor type $\nu_s(\mathrm{CCO}_d)$ symmetric valence vibration. Further increases in the ethanol concentration lead to a sharp drop in the number of dimers, as well as of monomers, and the double absorption band degenerates into a single band.

[a)]Email: Andrei.Drobyshev@kaznu.kz

[1]G. E. Gibson, G. S. Parks, and W. M. Latimer, J. Am. Chem. Soc. **42**, 1542 (1920).
[2]O. Haida, H. Suga, and S. Seki, J. Chem. Thermodyn. **9**, 1133 (1977).
[3]M. Ramos, S. Viera, F. Bermejo, J. Davidowski, H. Fischer, H. Schober, H. Gonzales, C Loong, and D. Price, Phys. Rev. **78**, 82 (1997).
[4]C. Talon, M. Ramos, S. Viera, G. Guello, F. Bermejo, A. Griado, M. Senent, S. Bennington, H. Fischer, and H. Schober, Phys. Rev. B **58**, 745 (1998).
[5]C. Talon, M. Ramos, and S. Vieira, Phys. Rev. B **66**, 012201 (2002).
[6]A. Aldiyarov, M. Aryutkina, A. Drobyshev, and M. Kurnosov, Fiz. Nizk. Temp. **35**, 333 (2009) [Low Temp. Phys. **35**, 251 (2009)].
[7]A. Drobyshev, A. Aldiyarov, D. Dzhumagaliuli, V. Kurnosov, and N. Tokmoldin, Fiz. Nizk. Temp. **33**, 627 (2007) [Low Temp. Phys. **33**, 472 (2007)].
[8]A. Drobyshev, A. Aldiyarov, D. Dzhumagaliuli, V. Kurnosov, and N. Tokmoldin, Fiz. Nizk. Temp. **33**, 479 (2007) [Low Temp. Phys. **33**, 355 (2007)].
[9]A. Drobyshev, K. Abdykalykov, A. Aldiyarov, V. Kurnosov, N. Tokmoldin, and D. Dzhumagaliuli, Fiz. Nizk. Temp. **33**, 916 (2007) [Low Temp. Phys. **33**, 699 (2007)].
[10]R. Larsen, Ph. Zielke, and M. Suhm, J. Chem. Phys. **126**, 194307 (2007).
[11]T. Wasserman and M. Suhm, J. Chem. Phys. A **114**, 8223 (2010).
[12]P. Zielke and M. Suhm, Phys. Chem. Chem. Phys. **8**, 2826 (2006).
[13]W. A. P. Luck and O. Schrems, J. Mol. Struct. **60**, 333 (1980).
[14]M. Oki and H. Iwamura, Bull. Chem. Soc. Jpn. **32**, 950 (1959).
[15]E. Gardner, A. Navarez, M. Garbalena, and W. Herndon, J. Mol. Struct. **784**, 249 (2006).
[16]H. L. Fang and R. L. Swofford, Chem. Phys. Lett. **105**(1), 5 (1984).
[17]S. Coussan, Y. Bouteiller, J. P. Perchard, and W. Q. Zheng, J. Phys. Chem. **102**, 578 (1998).
[18]A. A. Belhekar, M. S. Agashe, and C. I. Jose, J. Chem. Soc. Faraday Trans. **86**(10), 1781 (1990).
[19]Y. J. Hu, H. B. Fu, and E. R. Bernstein, J. Chem. Phys. **125**, 154305 (2006).
[20]L. Gonzales, O. Mo, and M. Yanez, J. Chem. Phys. **111**, 3855 (1999).
[21]M. Rozenberg, A. Loewenschuss, and Y. Marcus, Spectrochim. Acta A **53**, 1969 (1997).

Translated by D. H. McNeill